AIP | Review of Scientific Instruments

Grazing incidence extreme ultraviolet spectrometer fielded with time resolution in a hostile Z-pinch environment

K. M. Williamson, V. L. Kantsyrev, A. S. Safronova, P. G. Wilcox, W. Cline, S. Batie, B. LeGalloudec, V. Nalajala, and A. Astanovitsky

Citation: Review of Scientific Instruments **82**, 093506 (2011); doi: 10.1063/1.3626930
View online: http://dx.doi.org/10.1063/1.3626930
View Table of Contents: http://scitation.aip.org/content/aip/journal/rsi/82/9?ver=pdfcov
Published by the AIP Publishing

Grazing incidence extreme ultraviolet spectrometer fielded with time resolution in a hostile Z-pinch environment

K. M. Williamson, V. L. Kantsyrev, A. S. Safronova, P. G. Wilcox, W. Cline, S. Batie, B. LeGalloudec, V. Nalajala, and A. Astanovitsky
Plasma Physics and Diagnostics Laboratory, Physics Department, University of Nevada, Reno, Nevada 89557, USA

(Received 10 August 2010; accepted 1 August 2011; published online 28 September 2011)

This recently developed diagnostic was designed to allow for time-gated spectroscopic study of the EUV radiation (4 nm $< \lambda <$ 15 nm) present during harsh wire array z-pinch implosions. The spectrometer utilizes a 25 μm slit, an array of 3 spherical blazed gratings at grazing incidence, and a microchannel plate (MCP) detector placed in an off-Rowland position. Each grating is positioned such that its diffracted radiation is cast over two of the six total independently timed frames of the MCP. The off-Rowland configuration allows for a much greater spectral density on the imaging plate but only focuses at one wavelength per grating. The focal wavelengths are chosen for their diagnostic significance. Testing was conducted at the Zebra pulsed-power generator (1 MA, 100 ns risetime) at the University of Nevada, Reno on a series of wire array z-pinch loads. Within this harsh z-pinch environment, radiation yields routinely exceed 20 kJ in the EUV and soft x-ray. There are also strong mechanical shocks, high velocity debris, sudden vacuum changes during operation, energic ion beams, and hard x-ray radiation in excess of 50 keV. The spectra obtained from the precursor plasma of an Al double planar wire array contained lines of Al IX and AlX ions indicating a temperature near 60 eV during precursor formation. Detailed results will be presented showing the fielding specifications and the techniques used to extract important plasma parameters using this spectrometer. [doi:10.1063/1.3626930]

I. INTRODUCTION

The extreme ultraviolet (EUV) and soft x-ray (SXR) spectral regions (4 nm $< \lambda <$ 15 nm) are rich in atomic transitions that are of particular diagnostic importance for research in laser plasma sources, inertial and magnetic confinement fusion, and pulsed power physics. Time-resolved spectroscopic investigation is often the only source of information on electron temperature and density, charge state, and magnetic field; plasma parameters crucial to the study of dynamic flows and interactions.

EUV spectrometers are a staple in magnetically confined plasma studies,[1–3] particularly for the investigation of plasma impurities, but it is rarely used in inertially confined plasmas produced using large electrical generators, such as z-pinch or multibeam laser facilities, due to the risk of damaging the spectroscopic components.[4] Established EUV spectrometer designs, such as SPRED,[5] XUES,[6] and SFFS,[2] utilize flat field focusing gratings for obtaining spectra with various bandwidth and resolution parameters. In contrast, the spectrometer under discussion utilizes three spherical gratings along with Rowland focusing to capture the desired spectra.

While hostile-environment EUV/SXR spectroscopy can be challenging, it is a diagnostically useful tool in the study of high energy density climates, such as magnetically insulated transmission line plasma or z-pinch plasma.[4,7] The z pinch is a particularly challenging environment for fielding submicron filters and high-voltage multi-channel plate (MCP) detectors. University-scale z-pinch facilities are even being used to study the hostile environment of large multibeam laser facilities, such as the National Ignition Facility, used for fusion ignition research and other high energy-density science.[8] The new time-gated EUV (TGEUV) spectrometer was designed for long-term operation in such an environment in order to assess the electron temperature and density of the ablation phase of a wire array z pinch.

Every z-pinch load begins the experiment as a solid (wire arrays, liners) or as a gas (gas puff). As the pulsed-power-driver current flows through the load, it is ablated and ionized. This is particularly pronounced in wire array loads in which the ablation process gradually redistributed mass from solid wire cores to the axis over the majority of the current rise.[9] The ablation process can strongly affect the resulting pinch by seeding magneto hydrodynamic instabilities,[10] by influencing mass redistribution,[11] or by acting as a radiation source.[12] Time-gated EUV spectroscopy is crucial for the study of coronal plasma flows during the ablation phase of wire array z-pinch loads.

II. DESCRIPTION OF TIME-GATED, GRAZING-INCIDENCE SPECTROMETER

Z-pinch diagnostics must contend with harsh environments for each shot: high velocity debris, strong mechanical shocks, sudden vacuum changes during operation, energic ion beams, and hard x-ray radiation ($h\nu > 50$ keV). Combined with the submicron thin filters used for extreme ultraviolet filtering and the relatively long slit length (2.5 cm) required to create a long enough spectra to cover the face of a 4-cm-diameter MCP detector, these factors introduce several design challenges.

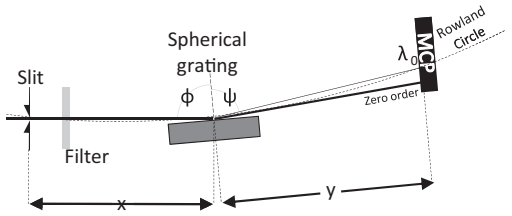

FIG. 1. Principle geometry of the off-Rowland, grazing-incidence spectrometer coupled with a MCP for time-resolved spectroscopy. The z-pinch radiation source is created to the left of the slit. The MCP can be shifted 6 cm under vacuum to capture different spectral regions. The focal wavelength λ_0 is located at the intersection of the Rowland circle with the MCP.

Experiments were performed using the Zebra generator at the University of Nevada Reno. This pulsed power generator routinely delivers 1.0 MA with 100 ns rise time to a load with 1.92 Ω pulse-forming line impedance. The typical dimensions of the z-pinch source at the time of interest were ~20 mm (anode-cathode gap) by 10 mm (array width). The TGEUV spectrometer was fielded 1.5 m from the source. A fast pneumatic gate valve between the slit and the source was used for high velocity debris mitigation during z-pinch experiments. This was used in conjunction with a manual gate valve to insure the high vacuum (10^{-6} torr) required to maintain an operational environment for the MCP. Strong mechanical shocks are avoided by coupling diagnostics to the chamber by flexible vacuum bellows and securing them to a mounting structure, which is not shocked during experiments. Hard x-ray radiation is prevented from reaching the MCP detector by the choice of the chamber housing the TGEUV: combined 7.5 cm of stainless steel. The weight of the chamber, in addition to the flexibility of the mounting apparatus, provides additional shock protection.

The principle of operation, shown in Figure 1, is the off-Rowland grazing-incidence geometry with time-resolved spectra recorded in a plane nearly perpendicular to the diffracted radiation. This off-Rowland scheme has the advantage of being simple to align, robust in operation, and able to capture a large spectral range within a relatively small solid angle. However, focus can only be achieved for precisely one wavelength λ_0 per grating, corresponding to the intersection of the MCP with the Rowland circle. Adjustment of λ_0 is performed geometrically by changing the slit-to-grating distance and the grating angle according to the grating equation and Rowland focusing geometry (MCP-to-grating distance is fixed). The minimum wavelength that can be imaged at grazing angle $\lambda_{min} = 6.7\varphi$ (Ref. 13) is near 40 Å for this device. In practice, the spectrometer is adjusted such that the focal wavelength coincides with diagnostically important transitions.

Frame (a) of Figure 2 shows the assembled device, which is decagonal, 10 cm deep, and 33 cm across. The exit port to which the MCP (a6) is mounted is a flexible bellows cut into the corner opposing (164°) the radiation entrance port. This feature provides 6 cm of rough translation for the MCP while under vacuum. During operation, a turbo pump is mounted on the chamber cover with other vacuum gauges and valves

(a)

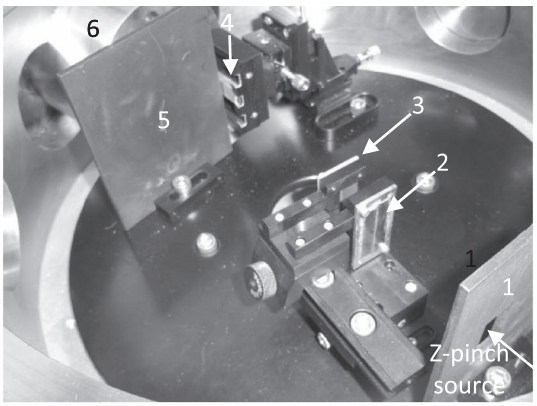

(b)

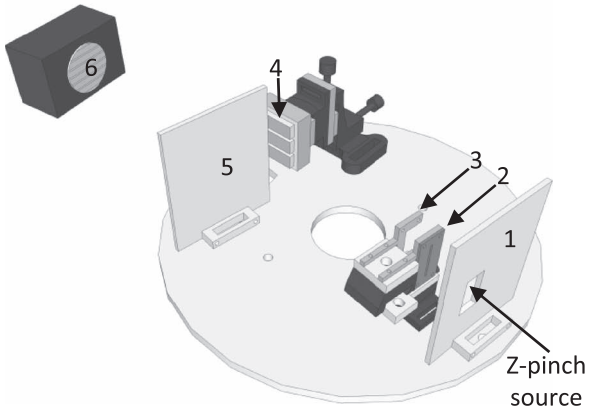

FIG. 2. Time-gated, EUV spectroscopy diagnostic based on the off-Rowland grazing incidence scheme: (a) picture of diagnostic elements: 1—front shield that limits incoming radiation to the size of the slit plate, 2—25 μm slit mounted on a rail and goniometer, 3—thin filter mount, 4—location of three gratings mounted on X–Z stage with goniometer, 5—light protection, 6—to six-frame multichannel plate; and (b) illustration of diagnostic with numbered elements matching (a).

mounted on the unused ports. The additional turbo pump provides differential pumping during operation to maintain high vacuum for the MCP during the sudden vacuum changes that occur each shot.

The spectrometer elements are illustrated in Figure 2(b). The incoming radiation is first reduced to a rectangle smaller than the slit plate by an anodized light baffel (1). The slit used in these experiments was 0.0025 cm by 2.5 cm (2). Immediately following is the aligned filter mount (3) with a custom 0.146 μm Zr filter from Luxel Corp. This filter is stabilized using a thin Ni mesh across a 0.005 cm × 2.5 cm gap with only cross-gap wires in the transmission region. The slit and filter plates are mounted onto an optical rail coupled to a fine-adjustment goniometer. The virtual axis of rotation is at the center of the slit and filter parallel to the optical path.

Three spherical gratings can be used (4). The separation of each grating was designed to cast spectra over

TABLE I. Parameters for configuration used to produce experimental spectum in Figure 4.

Spectrometer parameters	
Grove density (mm^{-1})	1200
Blaze angle (°)	2
Spectral range (nm)	3–300
Incidence angle (°)	84.25 ± 0.05
Blaze wavelength (nm)	6
Grating radius (m)	1.0
Experimental resolution $\lambda/\Delta\lambda$	300

two frames of the MCP detector, allowing for greater flexibility in the spectral or time region to be imaged. The grating mount surfaces were modified with 10° inclines to reflect slit radiation incident between the gratings away from the MCP. Another fine-adjustment goniometer is employed atop a fine-adjustment x–z stage, such that the virtual axis of rotation is at the midpoint of the gratings. The entire stage is neutrally mounted at 8° from the incoming radiation to reduce the required range of the goniometer. The clips used to hold the gratings in place (seen in Figure 2(a) but not shown in Figure 2(b) for clarity) were designed with a ~1 mm raised front edge to cast a shadow over the face of the clip at the desired angle of operation to eliminate reflections to the MCP. Additionally, the source-side clip is cutout at the center of each grating to allow for a lower angle of incidence and a higher efficiency. The final light protection (5) is fixed within several mm of the grating face to ensure that direct light is unable to reach the MCP (6) during operation. Film was used to record the MCP data.

III. APPLICATION

The purpose of this spectrometer is to assess the plasma conditions of a wire-array z-pinch precursor. Specifically of interest is the electron temperature of the secondary precursor structures observed with double-planar wire arrays[14,15] in order to benchmark magneto hydrodynamic simulation codes and better understand the resulting implosion dynamics of this load.

Figure 3 shows the current, time history of plasma emission, and TGEUV timing signal from Zebra shot #2164 (Al double planar wire array). The wavelength for 10% transmission λ_{10} for the EUV diode is 200 nm (0.2 μm Al + 50 μm pinhole), for the XRD diode λ_{10} is 6.8 nm (5 μm Kimfoil), and for the PCD diode λ_{10} is 1.6 nm (8 μm Be). The spectrum, see Table I, was captured with a 1200 groove/mm W/Re blazed grating with 4 ns exposure 50 ns prior to peak output: during the time of precursor formation.

A non-local thermal equilibrium (non-LTE) kinetic model of Al was used to produce synthetic spectra at various plasma conditions and to identify the most prominent Al EUV spectral features in the 5.0–6.5 nm wavelength range.[16] The complete atomic energy level structures, radiative, and collisional coupling data were calculated using the Flexible Atomic Code (FAC).[17] The FAC includes the ground states of all ions, from neutral to bare nucleus, and depends on the

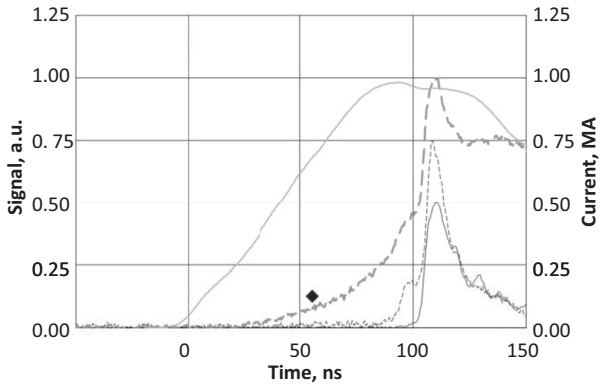

FIG. 3. Experimental data for Zebra shot 2164, DPWA Al (5056), interplanar gap 6 mm, linear mass density is 66 μg/cm, and aspect ratio is 1.1. Experimental signals: current (thick grey), EUV (thick dashed grey), XRD (dashed black), PCD (solid black), and time-gated EUV spectrometer timing signal (black diamond).

plasma conditions (T_e, N_e). The energy levels are fully coupled by radiative decay and radiative recombination, collisional excitation and ionization, Auger decay and their inverse rates.

The experimental spectrum is shown in Figure 4 was set to focus at 6 nm due to the first-order, low-spectral-density of temperature sensitive transitions expected there. The most prominent ionization stages, Al IX and Al X, of this spectrum were modeled and summarized in Table II. The Al IX and Al X transitions dominate the spectrum, which indicates an electron temperature of 60 eV with an approximately electron density of 10^{19} cm^{-3}.

An electron temperature of 60 eV is consistent with the emission data. The bulk plasma radiation was detected by the

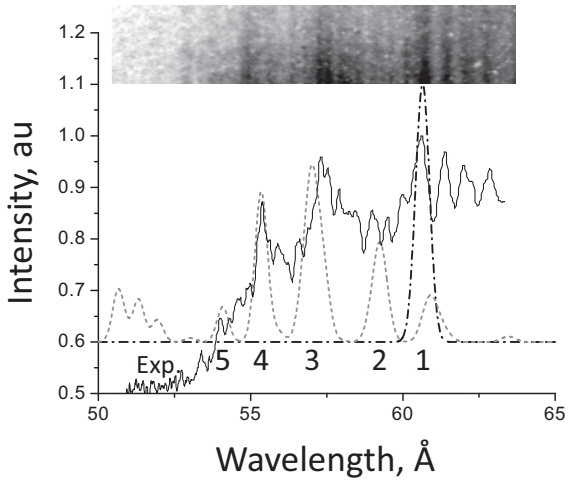

FIG. 4. Shot 2164 DPWA Al (5056), interplanar gap 6 mm, linear mass density is 66 μg/cm, and aspect ratio is 1.1. Experimental time-gated EUV spectra from –50 ns relative to peak XRD power superimposed at the top with lineout graphed below in the same scale (solid black). Relevant synthetic spectra from Al IX (dashed grey) and Al X (dashed black). Modeled transitions are numbered 1–5 (see Table II).

TABLE II. Summary of atomic transitions identified and numbered in Figure 4. Wavelengths under FAC refer to the results of the Flexible Atomic Code (FAC) (Ref. 15) for comparison with tabulated values from the National Institute of Standards and Technology (NIST) (Ref. 18).

		Wavelength (Å)		
Line no.	Transitions	FAC I	NIST	Ions
1	$1s^2 2s 2p^2 {}^4P_{5/2}–1s^2 2s 2p 3d {}^4D_{7/2}$	60.63	60.59	Al IX
2	$1s^2 2s 2p {}^1P_1–1s^2 2s 3d {}^1D_2$	59.21	59.11	Al X
3	$1s^2 2p^2 {}^1D_2–1s^2 2p 3d {}^1F_3$	57.06	57.37	Al X
4	$1s^2 2s 2p^3 P_2–1s^2 2s 3d {}^3D_3, {}^3D_2$	55.34	55.38	Al X
5	$1s^2 2s 2p {}^1P_1–1s^2 2p 3p {}^1D_2$	54.29	54.12	Al X

EUV diode between 17 and 200 nm. The ion transitions, between 5 and 6.5 nm, falls onto the lower sensitivity limit of the XRD diode with ~15% transmission. At peak output, the XRD is expected to register powers of hundreds of gigawatts. The combination of low filter transmission, low XRD sensitivity, and relatively low-power line transitions explain the inconclusive XRD signal.

IV. CONCLUSION AND FUTURE WORK

A new, time-gated spectrometer based on the off-Rowland grazing-incidence scheme was designed and successfully tested under harsh conditions at the Zebra z-pinch facility. The experimental time-gated Al spectrum, shown herein, was calibrated and modeled using a non-LTE kinetic code. The results of modeling indicate an electron temperature and density of $T_e = 60$ eV and $N_e = 10^{19}$ cm^{-3}, respectively, during the precursor formation of an Al double planar wire array.

Future work on this diagnostic should include the testing of additional gratings to fully utilize the six-frame MCP. An additional permanent magnet placed between the plasma source and the slit would provide shielding from energetic, charged particles and prolong the life of the filter. Further customization and calibration of the rough translation MCP mount would allow for wider operational range while maintaining vacuum. The design could also be modified to accomidate flat field focusing gratings.

ACKNOWLEDGMENTS

This work was supported by DOE/NNSA cooperative agreements DE-FC52-06NA27586, DE-FC52-06NA27588, and in part DE-FC52-06NV27616.

[1] B. C. Stratton, M. Bitter, K. W. Hill, D. L. Hillis, and J. T. Hogan, Fusion Sci. Technol. **53**, 431 (2008).
[2] J. Clementson, P. Beiersdorfer, and E. W. Magee, Rev. Sci. Instrum. **79**, 10F538 (2008).
[3] P. Beiersdorfer, J. K. Lepson, M. Bitter, K. W. Hill, and L. Roquemore, Rev. Sci. Instrum. **79**, 10E318 (2008).
[4] V. L. Kantsyrev, A. S. Safronova, K. M. Williamson, P. Wilcox, N. D. Ouart, K. W. Struve, D. L. Voronov, R. M. Feshchenko, I. A. Artyukov, and A. V. Vinogradov, Rev. Sci. Instrum. **79**, 10F542 (2008).
[5] B. C. Stratton, R. J. Fonck, K. Ida, K. P. Jaehnig, and A. T. Ramsey, Rev. Sci. Instrum. **57**, 2043 (1986).
[6] P. Beiersdorfer, M. Bitter, L. Roquemore, J. K. Lepson, and M. F. Cu, Rev. Sci. Instrum. **77**, 10F306 (2006).
[7] A. P. Shevelko, D. E. Bliss, E. D. Kazakov, M. G. Mazarakis, J. S. McGurn, L. V. Knight, K. W. Struve, I. Yu. Tolstikhina, and T. J. Weeks, Plas. Phys. Rep. **34**, 944 (2008).
[8] J. M. Kindel, Stewardship Science Academic Aliance (SSAA) Presentation, Jan. 20 (2010), http://www.orau.gov/ssaas2010/presentations/kindel.pdf.
[9] S. V. Lebedev, F. N. Beg, S. N. Bland, J. P. Chittenden, A. E. Dangor, M. G. Haines, K. H. Kwek, S. A. Pikuz, and T. A. Shelkovenko, Phys. of Plasmas **8**, 3734 (2001).
[10] S. N. Bland, S. V. Lebedev, J. P. Chittenden, G. N. Hall, F. Suzuki-Vidal, D. J. Ampleford, S. C. Bott, J. B. A. Palmer, S. A. Pikuz, and T. A. Shelkovenko, Phys. of Plasmas **14**, 056315 (2007).
[11] K. M. Williamson, V. L. Kantsyrev, A. A. Esaulov, A. S. Safronova, N. D. Ouart, F. M. Yilmaz, I. K. Shrestha, V. Shlyaptseva, R. D. McBride, D. A. Chalenski, J. D. Douglass, J. B. Greenly, D. A. Hammer, and B. R. Kusse, Phys. Plasmas **16**, 012704 (2009).
[12] S. C. Bott, S. V. Lebedev, D. J. Ampleford, S. N. Bland, J. P. Chittenden, A. Ciardi, M. G. Haines, C. Jennings, M. Sherlock, G. Hall, J. Rapley, F. N. Beg, and J Palmer, Phys. Rev. E **74**, 046403 (2006).
[13] W. Lochte-Holtgreven, *Plasma Diagnostics* (Amsterdam, North-Holland Publishing, 1968).
[14] V. L. Kantsyrev, L. I. Rudakov, A. S. Safronova, A. A. Esaulov, A. S. Chuvatin, C. A. Coverdale, C. Deeney, K. M. Williamson, M. F. Yilmaz, I. Shrestha, N. D. Ouart, and G. C. Osborne, Phys. Plasmas **15**, 030704 (2008).
[15] K. M. Williamson, V. L. Kantsyrev, A. A. Esaulov, A. S. Safronova, P. Cox, I. Shrestha, G. C. Osborne, M. E. Weller, N. D. Ouart, and V. V. Shlyaptseva, Phys. Plasmas **17**, 112705 (2010).
[16] A. S. Safronova, V. L. Kantsyrev, A. A. Esaulov, N. D. Ouart, M. F. Yilmaz, K. M. Williamson, I. Shrestha, G. C. Osborne, J. B. Greenly, K. M. Chandler, R. D. McBride, D. A. Chalenski, D. A. Hammer, B. R. Kusse, and P. D. LePell, Physics of Plasmas **15**, 033302 (2008).
[17] M. F. Gu, Can. Journ. Phys. **86**, 675 (2008).
[18] NIST Atomic Spectral Database: http://physics.nist.gov/asd3